SLP Presentation

Laboratory Studies of Cosmology-Inspired Defect Dynamics in Liquid Crystals

Anik Mandal
SLP Guide : Prof. Pramoda Kumar
PhD Supervisor : Prof. Somak Raychaudhury

January 22, 2026

Ashoka University, Sonipat

Symmetry and Symmetry Breaking

Symmetry	Broken Symmetry
Condition: Cat isn't hungry	Condition: Cat is hungry
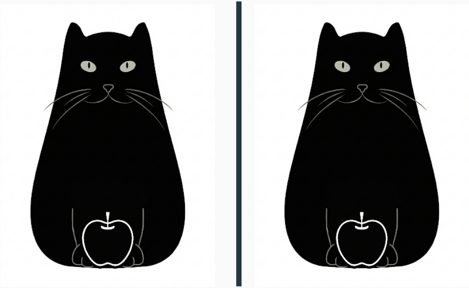	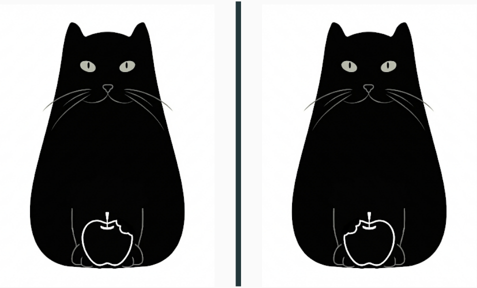

- Early Universe evolution involves a hierarchy of symmetry-breaking events.[1,2]

[1] Kibble (1982) *Acta Phys. Polon. B* 13 p. 723

[2] Vilenkin (1985) DOI: 10.1016/0370-1573(85)90033-X

Formation of Topological Defects

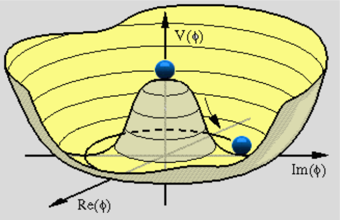

(a) Symmetry Breaking (Source)

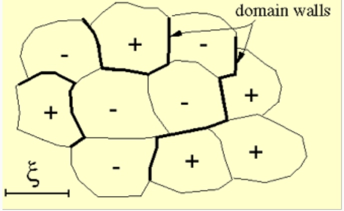

(b) Domain Walls (Source)

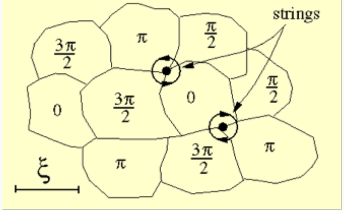

(c) String Defects (Source)

- Defect or mismatch forms at the boundary of two causally disconnected points in space.[3]
- Cosmological defects acted as gravitational seeds for large-scale structure, drove CMB anisotropies, and remain viable candidates for dark matter.

[3] Kibble (1976) DOI: 10.1088/0305-4470/9/8/029

Cosmology in the Laboratory

- In 1985, Zurek extended Kibble's idea to condensed matter physics.[4,5]
- Liquid crystals adopted as a robust alternative.[6,7,8]

[4] Zurek (1985) DOI: 10.1038/317505A0
[5] Zurek (1996) DOI: 10.1016/S0370-1573(96)00009-9
[6] Chuang et al. (1991) DOI: 10.1126/SCIENCE.251.4999.1336
[7] Yurke et al. (1992) DOI: 10.1016/0921-4526(92)90179-V
[8] Fowler and Dierking (2017) DOI: 10.1002/CPHC.201700023

Kibble-Zurek Mechanism | Project Objectives

- Kibble–Zurek scaling of defect density (ρ),

$$\rho \propto \tau_Q^{-d\nu/(1+\nu z)},$$

  - Critical slowing down near the transition point.
  - system freezes at certain time and length scale.

- Defect networks coarsen to minimize the Frank elastic free energy,

$$F = \frac{1}{2}\left[K_1(\nabla\cdot\mathbf{n})^2 + K_2(\mathbf{n}\cdot\nabla\times\mathbf{n})^2 + K_3|\mathbf{n}\times\nabla\times\mathbf{n}|^2\right],$$

  - String defect (d=2) : $\rho(t) \propto t^{-1}$
  - Domain walls (d=1) : $\rho(t) \propto t^{-1/2}$

Experimental Setup

- Patterning
- Etching
- Post etching treatment
- Applying surfactant (DMOAP)
- Cell assembly
- Cell thickness measurement
- LC filling and cooling

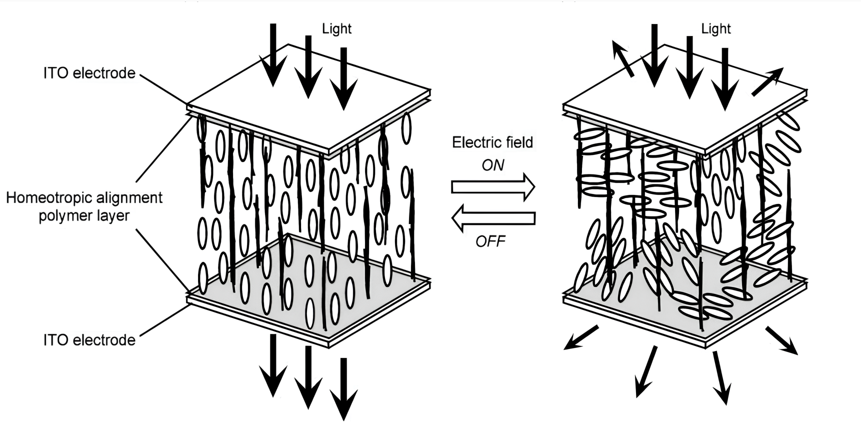

Fréedericksz transition due to electric field quench in homeotropically aligned LC (Source)

Preparing Homeotropic Cell

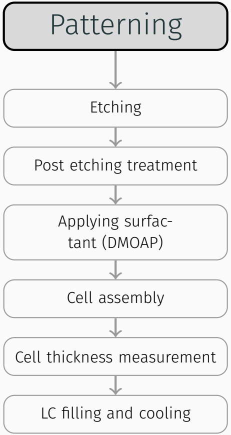

- ITO-coated glass cut to $4 \times 2\,\mathrm{cm}^2$.
- Conductive side identified using a multimeter.
- Cello tape masks $1\,\mathrm{cm}$ electrode region, leaving $0.5\,\mathrm{cm}$ gaps at both ends.

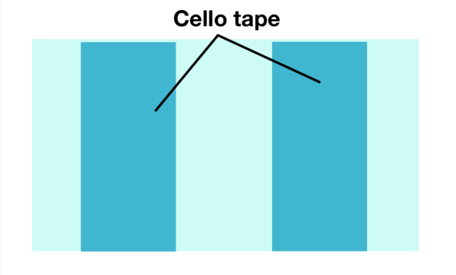

Patterning

Preparing Homeotropic Cell

- Patterning
- **Etching**
- Post etching treatment
- Applying surfactant (DMOAP)
- Cell assembly
- Cell thickness measurement
- LC filling and cooling

- Etching solution: concentrated HCl + Zn powder.
- Exposure time: 30 minutes (inside fume hood).
- Removes unprotected ITO, leaving defined electrodes.
- Rinsed with water and dilute base to neutralize acid.

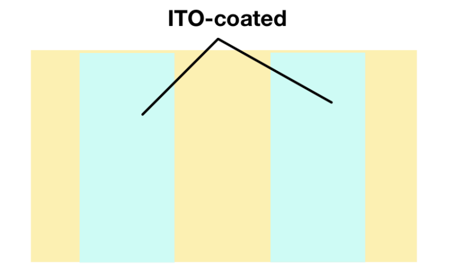

Eatching

Preparing Homeotropic Cell

- Patterning
- Etching
- **Post etching treatment**
- Applying surfactant (DMOAP)
- Cell assembly
- Cell thickness measurement
- LC filling and cooling

- Etched glass cut into two symmetric electrode slabs.
- Manual scrubbing with soap and IPA removes loose residues.
- Ultrasonic cleaning: Soap-water bath for 15 minutes at 40-50°C
- Final rinse with fresh IPA and dried using nitrogen gas to prevent streaking or residue.

Preparing Homeotropic Cell

Patterning
↓
Etching
↓
Post etching treatment
↓
Applying surfactant (DMOAP)
↓
Cell assembly
↓
Cell thickness measurement
↓
LC filling and cooling

- 0.2% DMOAP solution prepared in distilled water. Glass slabs were dipped vertically for 5 minutes.
- Methoxy groups hydrolyze and bind to surface hydroxyl groups.
- Subsequent baking at 110°C for 60 minutes forms strong covalent siloxane (Si-O-Si) bonds, and molecules orient perpendicular to the substrate.

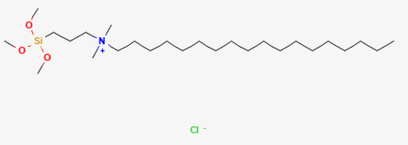

(a) DMOAP (Source)

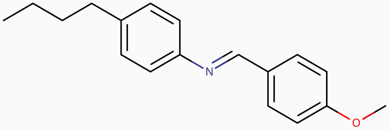

(b) MBBA (Source)

Preparing Homeotropic Cell

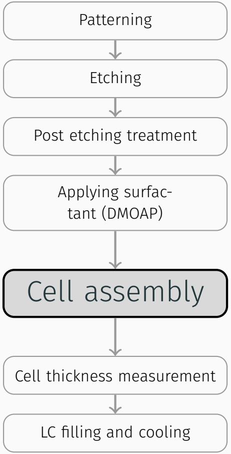

- DMOAP-treated slabs are sandwiched together along with 23 μm Mylar film, placed along the edges.
- Applied gentle pressure (30 min), then epoxy cured (24 h).
- Conducting wires soldered to ITO electrodes using Indium.

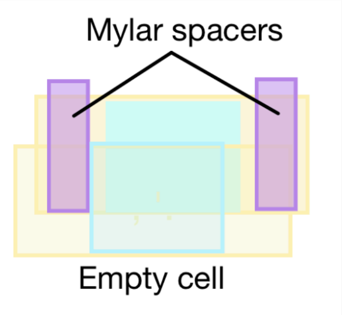

Cell assembly

Preparing Homeotropic Cell

- Patterning
- Etching
- Post etching treatment
- Applying surfactant (DMOAP)
- Cell assembly
- **Cell thickness measurement**
- LC filling and cooling

▶ Measured capacitance (C) using LCR meter; modeled as parallel plates to measured cell thickness.

$$d = \frac{\varepsilon_0 \varepsilon_r A}{C}$$

▶ Measured thickness:

- 1st cell : $31.09 \pm 0.44\ \mu m$
- 2nd cell : $43.62 \pm 2.18\ \mu m$

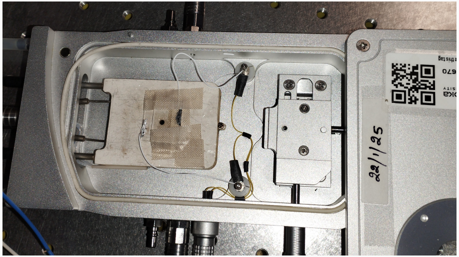

Cell placed in a temperature-controlled stage system

Preparing Homeotropic Cell

Patterning
↓
Etching
↓
Post etching treatment
↓
Applying surfactant (DMOAP)
↓
Cell assembly
↓
Cell thickness measurement
↓
LC filling and cooling

Thermal Protocol

1. Heat to 50°C @ 20°C/min, hold 10 min
2. Cool to 36°C @ 1°C/min, hold 5 min
3. Cool to 25°C @ 0.1°C/min

- MBBA introduced at elevated temperature.
- Capillary action fills the cell uniformly.
- Slow cooling minimizes permanent defect formation.

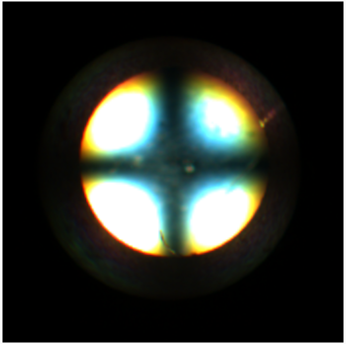

Conoscopic image confirms Homeotropic alignment

Final Setup

- 10-60 V RMS, 10 kHz sine wave electric field has been generated using a *function generator* and *A800DI amplifier* and provided to the cell.

- Data taken at 28°Cm controlled temp; 10× optical magnification.
- Video recorded at 100 fps under polarized illumination.

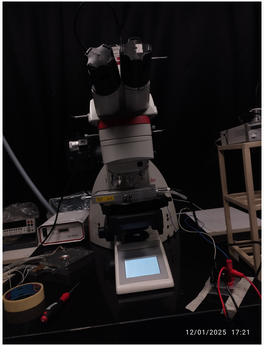

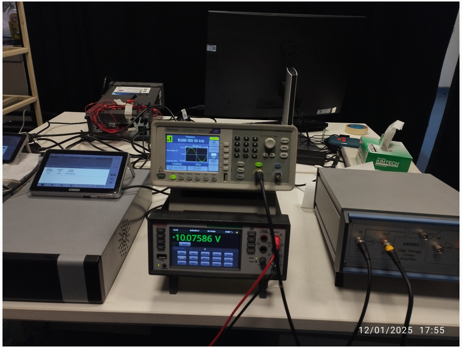

Computational Framework[9]

- Pre-processing and noise reduction
- ↓
- Ridge detection
- ↓
- Hysteresis thresholding
- ↓
- Binary closing and cleaning
- ↓
- Skeletonizing
- ↓
- Estimating defect density

▶ Developed an automated image processing pipeline to quantify defect density frame-by-frame.

[9] Clone: $ git clone https://github.com/mandal-anik10/SLP-CosmoWithLCs.git

Computational Framework

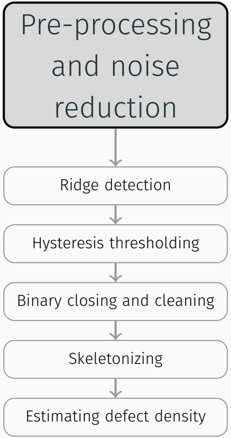

- 3×3-median filter suppresses impulsive noise by replacing each pixel value with the median of its 3×3 neighborhood.
- Preserves sharp edges and fine structural details better than linear filters.

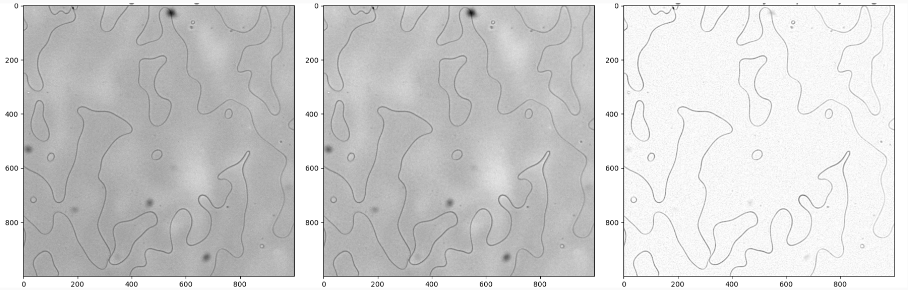

(L) Original, (C) Denoised, (R) Ridge Map

Computational Framework

Pre-processing and noise reduction

↓

Ridge detection

↓

Hysteresis thresholding

↓

Binary closing and cleaning

↓

Skeletonizing

↓

Estimating defect density

- Applied modified Hessian-based Meijering[a] ridge detection filter.
- A modified Hessian matrix was constructed as

$$H'_f(x) = \begin{bmatrix} f_{xx} + \alpha f_{yy} & (1-\alpha) f_{xy} \\ (1-\alpha) f_{xy} & f_{yy} + \alpha f_{xx} \end{bmatrix}.$$

  Where $f_{ij}(x, y) = (f * \frac{\partial^2 G}{\partial_i \partial_j})(x, y)$, for the image f and normalized Gaussian kernel G, $\alpha = 1/3$ for 2D image.
- Eigenvalues of $H'_f(x)$ were used to compute a "neuriteness" measure per pixel.
- The eigenvector corresponding to the smaller absolute eigenvalue(≥ 0) defines the local ridge direction.

[a] Meijering et al. (2004) DOI: 10.1002/CYTO.A.20022

Computational Framework

- Pre-processing and noise reduction
- ↓ Ridge detection
- ↓ **Hysteresis thresholding**
- ↓ Binary closing and cleaning
- ↓ Skeletonizing
- ↓ Estimating defect density

▶ Applied hysteresis thresholds to suppress spurious ridges.

▶ Retained pixels $> Th_{\mathrm{high}}$, and those $> Th_{\mathrm{low}}$ only if connected to already-classified defect pixels through 8-connectivity neighborhoods.

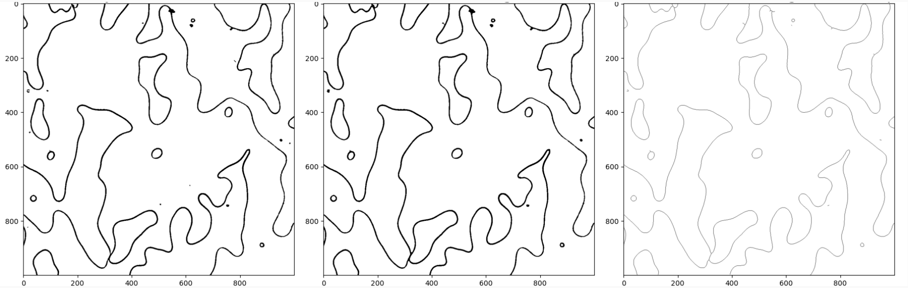

(L)Hysteresis threshold, (C)cleaned, (R) Skeletonized

Computational Framework

Pre-processing and noise reduction
↓
Ridge detection
↓
Hysteresis thresholding
↓
Binary closing and cleaning
↓
Skeletonizing
↓
Estimating defect density

- Applied binary closing to fill gaps and ensure defect line continuity.
- Eliminated isolated noise and fragments via a minimum length threshold.

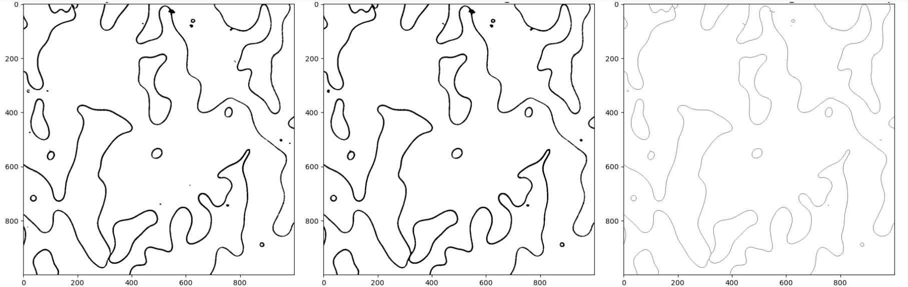

(L)Hysteresis threshold, (C)cleaned, (R) Skeletonized

Computational Framework

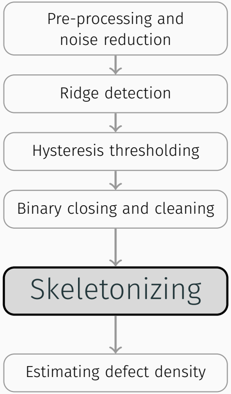

- Applied morphological thinning to collapse wide defect regions into their fundamental medial axis.
- Preserves the object's topology and connectivity, ensuring the skeleton represents the original structure.

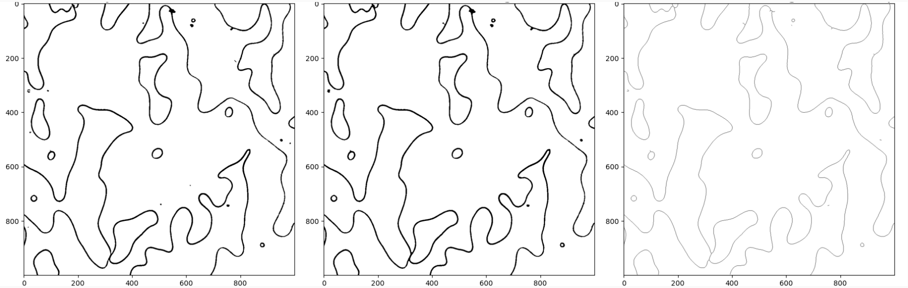

(L)Hysteresis threshold, (C)cleaned, (R) Skeletonized

Computational Framework

Pre-processing and noise reduction
↓
Ridge detection
↓
Hysteresis thresholding
↓
Binary closing and cleaning
↓
Skeletonizing
↓
Estimating defect density

- Total defect length computed by summing the lengths of all skeleton branches.
- Defect density derived by dividing the total length by the sample volume (V), given by $\rho = L/V$.

Error Analysis: Temporal Uncertainty

- $\sim 30\%$ frame drop at 100 fps (write-speed limit) caused non-uniform temporal distortion.
- Reconstruct a statistically true timeline using Monte Carlo resampling.

Monte Carlo Time Correction

- Resampled frame sequence 1000 times with 100/70 time rescaling to account for the frame drops.
- Defined corrected timestamp as:

$$t_i = \mu_{t_i} \pm \sigma_{t_i}$$

- Median μ_{t_i} used as true time of the frames; σ_{t_i} tracks uncertainty[10].

[10] Horizontal error bars omitted from the plots for visual clarity

Error Analysis: Systematic Error in Defect Density

1. Error in area measurement (5%)
   - Error of $2\,\mathrm{mm}$ in unit length $\Rightarrow 4\,\mathrm{mm}^2$ error in area ($A = 80\,\mathrm{mm}^2$).
   - Propagates linearly to density:

$$\frac{d\rho}{\rho} \approx \frac{dA}{A} \approx 5\%$$

2. Error in calibration scale (0.3%)
   - Scale bar ($1174\,\mathrm{px}$) has edge width (1σ) uncertainty of $3.6\,\mathrm{px}$.
   - Propagates inversely ($\rho \propto C^{-1}$):

$$\frac{d\rho}{\rho} \approx \frac{dC}{C} = \frac{3.6}{1174} \approx 0.3\%$$

Total Systematic Uncertainty: 5.3%

Error Analysis: Stochastic error in defect density

- Quantified stochastic error via mean ($\bar{x}$) and standard deviation(σ) of independent trials ($N = 5$, for defect formation $N = 3$).

$$x = \bar{x} \pm \sigma = \frac{1}{N}\sum_{i=1}^{N} x_i \pm \sqrt{\frac{\sum_{i=1}^{N}(x_i - \bar{x})^2}{N-1}}$$

- **Relative error selection criteria:** 20-point median of relative errors

$$median\left(\frac{\sigma}{\bar{x}}(t)\right) < 0.1$$

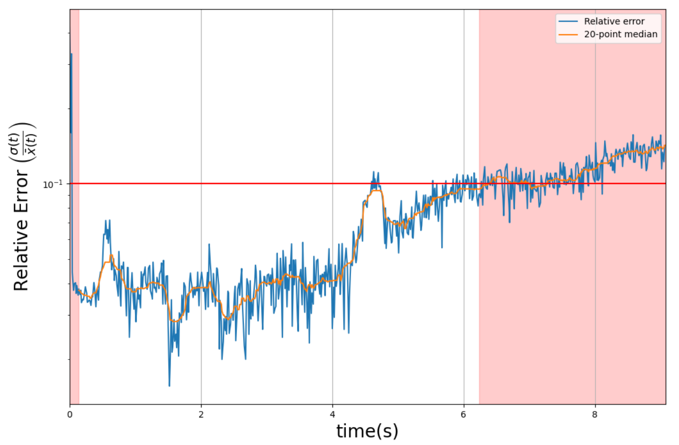

This example figure (60V data) shows the region selected based on the selection criteria.

Late time dynamics: cell with permanent defects

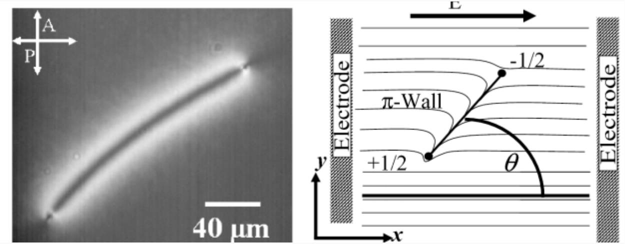

(L) A pair of ±1/2 wedge disclinations connected by a π-wall under a cross polarizer. (R) 2D director field Sketch (Source[a])

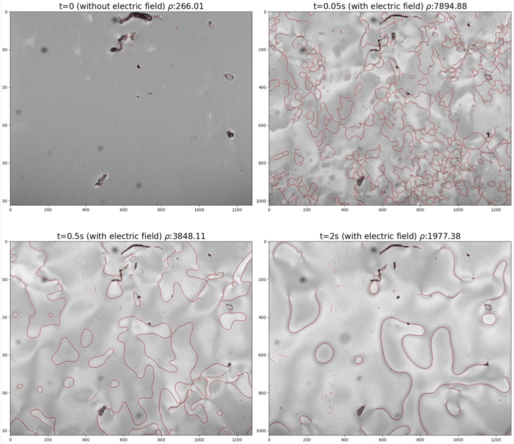

Topological defects at different time stamps for 60V at 10× resolution.

[a] Blanc et al. (2005) DOI: 10.1103/PhysRevLett.95.097802

Late time dynamics: cell with permanent defects

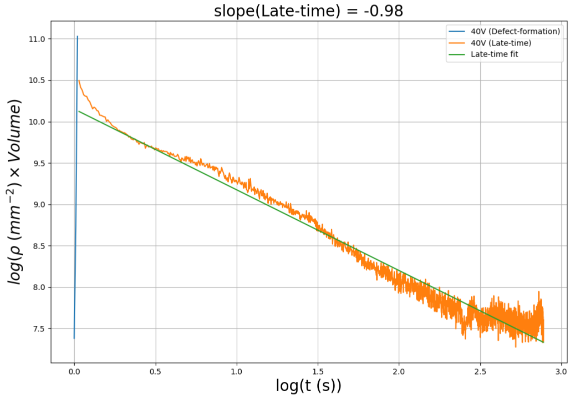

(a) 40V : -0.98

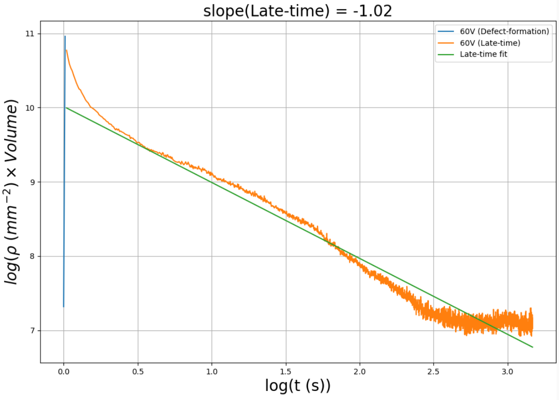

(b) 60V : -1.02

Late time dynamics: cell with permanent defects

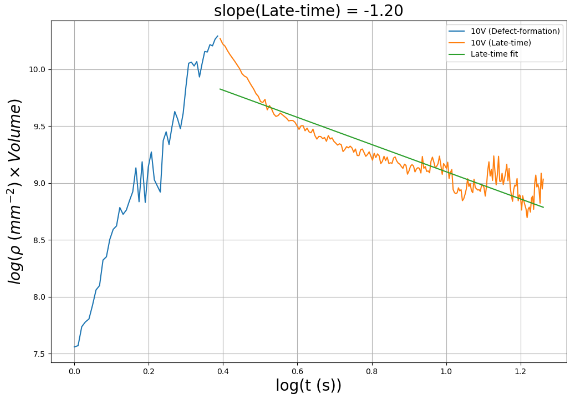

(c) 10V : -1.20

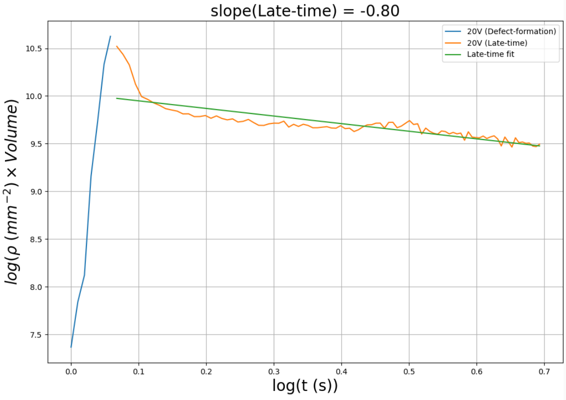

(d) 20V : -0.80

Late time dynamics: cell without permanent defects

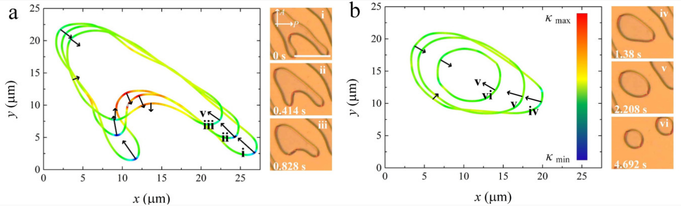

Shape evolution of a single domain at different moments and the corresponding polarizing optical microscope micrographs. (L) Early stage of annihilation (R) Late stage of the annihilation(Source[a])

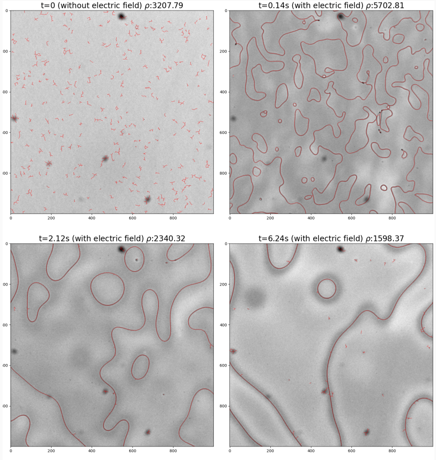

Topological defects at different time stamps for 60V at 10× resolution.

[a] Shen and Dierking (2020) DOI: 10.1016/J.MOLLIQ.2020.113547

Late time dynamics: cell without permanent defects

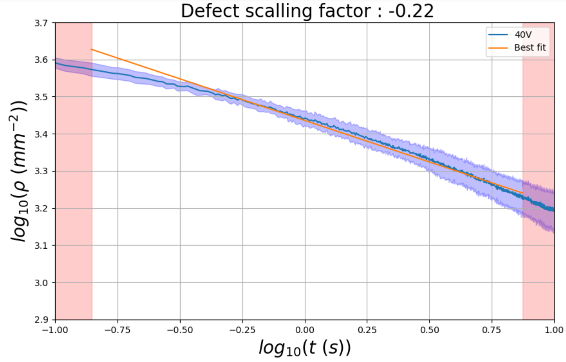

(a) 40V : -0.22

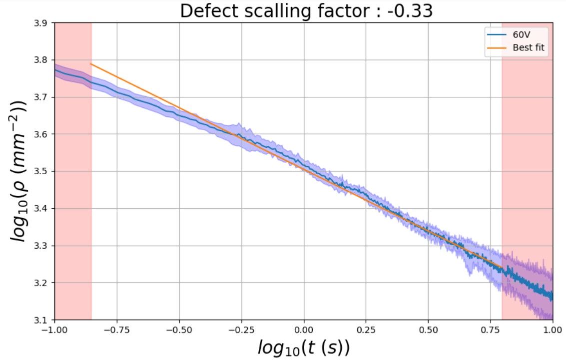

(b) 60V : -0.33[11,12]

[11] Guimarães et al. (2013) DOI: 10.1088/0953-8984/25/40/404203

[12] Dierking et al. (2025) DOI: 10.3390/CRYST15030214

Late time dynamics: cell without permanent defects

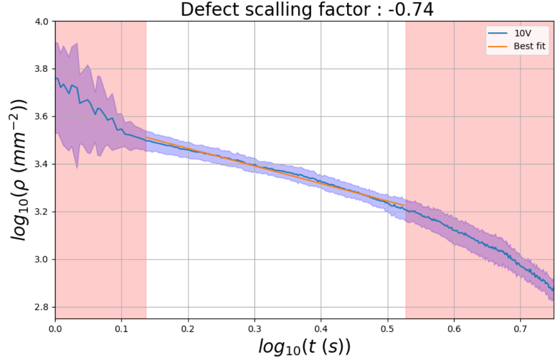

(c) 10V : -0.74

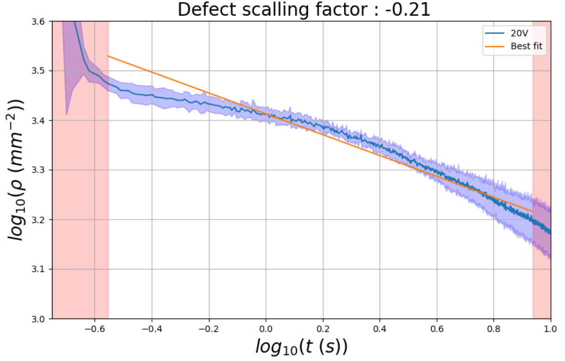

(d) 20V : -0.21

Formation dynamics

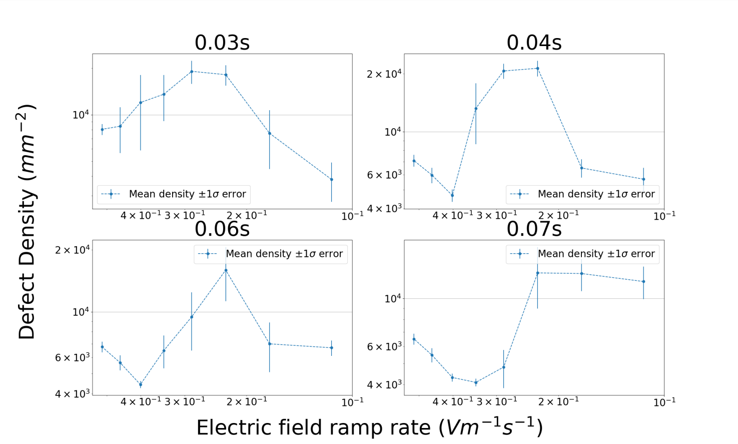

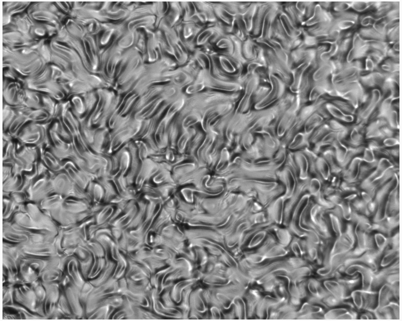

Electroconvection observed in the prepared MBBA LC at electric field frequency $\sim Hz$

Observed freeze-out of director dynamics and strong stochasticity at high electric field frequency(10Hz)

Conclusion

- **Late-Time Dynamics**
  - **Open Lines:** Defect density decays as $\rho(t) \propto t^{-1}$ (standard coarsening).
  - **Closed Loops:** Long-lived under strong E-fields; decay slower than tension models predict.
  - Variable π-wall widths observed, consistent with field-dependent coherence length.
- **Experimental Limits on KZM**
  - **High Freq ($10\,\mathrm{kHz}$):** Dielectric response is too slow; system freezes before critical dynamics.
  - **Low Freq:** Ion motion triggers electrohydrodynamic flow, disrupting ordered patterns.
  - *Result: No stable intermediate regime observed for KZM scaling of defects in MBBA LC.*

What people can learn next?

- **Future Directions**
  - Magnetic fields or rapid thermal quenches can be performed to access universal scaling with more suitable LCs like 5CB.
  - Inverse scaling of π-wall width vs. field strength can be verified.[13].
  - A more sophisticated machine-learning-based framework can be developed to resolve complex umbilic trajectories[14].
- **Questions I have**
  - Suppose vacuum states have non-degenerate masses; what effect would this asymmetry have on defect dynamics in the presence of gravity?
  - How does the probability of quantum tunneling between vacuum states (vacuum decay) influence the stability and evolution of the defect network?

[13] Blanc et al. (2005) DOI: 10.1103/PhysRevLett.95.097802
[14] Dierking et al. (2025) DOI: 10.3390/CRYST15030214

Acknowledgement

- Prof. Pramoda
- Ankit
- Prof. Somak and my SRC
- Shri Gowri, Kurshid da, my batchmates, and our small physics family
- Our family @TDI (Mainak Da, Debadyuiti Da, Arijit, Srijit Da, Susanta)

THANK YOU